J Periodontal Implant Sci. 2020 Apr;50(2):106-120
https://doi.org/10.5051/jpis.2020.50.2.106
pISSN 2093-2278·eISSN 2093-2286

JPIS
Journal of Periodontal & Implant Science

Research Article
Implant Science

Check for updates

OPEN ACCESS

Received: Jul 6, 2019
Revised: Dec 22, 2019
Accepted: Feb 12, 2020

***Correspondence:**
Jintamai Suwanprateeb
Biofunctional Materials and Devices Research Group, National Metal and Materials Technology Center (MTEC), National Science and Technology Development Agency, 114 Paholyothin Road, Klong 1, Klongluang, Pathumthani 12120, Thailand.
E-mail: jintamai@mtec.or.th
Tel: +662-564-6500
Fax: +662-564-6446

ORCID iDs
Teerapan Sosakul
https://orcid.org/0000-0002-6339-2043
Pongsatorn Tuchpramuk
https://orcid.org/0000-0001-6899-5946
Waraporn Suvannapruk
https://orcid.org/0000-0001-9138-9418
Autcharaporn Srion
https://orcid.org/0000-0003-3133-8752
Bunyong Rungroungdouyboon
https://orcid.org/0000-0002-2475-5825
Jintamai Suwanprateeb
https://orcid.org/0000-0002-5555-3927

Evaluation of tissue ingrowth and reaction of a porous polyethylene block as an onlay bone graft in rabbit posterior mandible

Teerapan Sosakul [1], Pongsatorn Tuchpramuk [2], Waraporn Suvannapruk [3], Autcharaporn Srion [3], Bunyong Rungroungdouyboon [4], Jintamai Suwanprateeb [3,*]

[1]Department of Prosthodontics, Khon Kaen University Faculty of Dentistry, Khon Kaen, Thailand
[2]Office of Academic Affairs, Mahasarakham University Faculty of Veterinary Sciences, Maha Sarakham, Thailand
[3]Biofunctional Materials and Devices Research Group, National Metal and Materials Technology Center (MTEC), National Science and Technology Development Agency, Pathumthani, Thailand
[4]Department of Mechanical Engineering, Thammasat University Faculty of Engineering, Pathumthani, Thailand

ABSTRACT

Purpose: A new form of porous polyethylene, characterized by higher porosity and pore interconnectivity, was developed for use as a tissue-integrated implant. This study evaluated the effectiveness of porous polyethylene blocks used as an onlay bone graft in rabbit mandible in terms of tissue reaction, bone ingrowth, fibrovascularization, and graft-bone interfacial integrity.
Methods: Twelve New Zealand white rabbits were randomized into 3 treatment groups according to the study period (4, 12, or 24 weeks). Cylindrical specimens measuring 5 mm in diameter and 4.5 mm in thickness were placed directly on the body of the mandible without bone bed decortication, fixed in place with a titanium screw, and covered with a collagen membrane. Histologic and histomorphometric analyses were done using hematoxylin and eosin–stained bone slices. Interfacial shear strength was tested to quantify graft-bone interfacial integrity.
Results: The porous polyethylene graft was observed to integrate with the mandibular bone and exhibited tissue-bridge connections. At all postoperative time points, it was noted that the host tissues had grown deep into the pores of the porous polyethylene in the direction from the interface to the center of the graft. Both fibrovascular tissue and bone were found within the pores, but most bone ingrowth was observed at the graft-mandibular bone interface. Bone ingrowth depth and interfacial shear strength were in the range of 2.76–3.89 mm and 1.11–1.43 MPa, respectively. No significant differences among post-implantation time points were found for tissue ingrowth percentage and interfacial shear strength (P>0.05).
Conclusions: Within the limits of the study, the present study revealed that the new porous polyethylene did not provoke any adverse systemic reactions. The material promoted fibrovascularization and displayed osteoconductive and osteogenic properties within and outside the contact interface. Stable interfacial integration between the graft and bone also took place.

Keywords: Bone-implant Interface; Bone regeneration; Histology; Interfacial shear strength; Polyethylenes; Rabbit

JPIS Journal of Periodontal & Implant Science

Author Contributions
Conceptualization: Teerapan Sosakul; Formal analysis: Teerapan Sosakul, Waraporn Suvannapruk, Autcharaporn Srion, Jintamai Suwanprateeb; Investigation: Teerapan Sosakul, Pongsatorn Tuchpramuk; Methodology: Teerapan Sosakul, Waraporn Suvannapruk, Autcharaporn Srion; Supervision: Bunyong Rungroungdouyboon, Jintamai Suwanprateeb; Writing - original draft: Teerapan Sosakul, Jintamai Suwanprateeb; Writing - review & editing: Bunyong Rungroungdouyboon, Jintamai Suwanprateeb.

Conflict of Interest
No potential conflict of interest relevant to this article was reported.

INTRODUCTION

Augmentation of alveolar bone defects or inadequate bone volume resulting from a broad range of causes, such as periodontal diseases, tooth extraction, and trauma or infection of the tooth, has frequently been performed to regain or restore the volume and the contour of the bone prior to dental implant placement. A technique that has been used for this purpose is bone grafting, which can be done using various types of materials. Currently, the use of autologous bone grafts is still considered to be the gold standard for alveolar bone regeneration, as autologous bone grafts possess osteoinductive, osteogenic, and osteoconductive properties that trigger new bone formation [1,2]. However, harvesting autologous bone, either intraorally or extraorally, could result in donor site morbidity, neurosensory disturbances, pain, increased operating time, temporary loss of function, and rapid graft resorption [3]. Alternatively, allogeneic grafts, which originate from living donors or cadaveric bone, or xenografts could be used, as these options do not require additional surgery for harvesting. However, allogenic grafts and xenografts pose a risk of an immunogenic reaction and transmission of infectious diseases, and must be processed to ensure their safety in a way that could affect their osteoinductive and osteoconductive potential [4,5]. As a result, several synthetic bone grafts have been developed and employed as alternatives to overcome these problems. Hydroxyapatite (HA) and biphasic HA/tricalcium phosphate ceramics are widely used types of synthetic grafts for bone replacement due to their good bioactivity and osteoconductive properties, but complications of these bioceramics still occur, such as brittleness, a poorly defined ridge, displacement to undesirable locations, and exposure of the submucosal layer to the oral cavity [6,7].

Porous polyethylene implants have been successfully used in several applications, such as cranial reconstruction, nasal reconstruction, ear reconstruction, orbital reconstruction, and correction of maxillofacial contour deformities because of their biocompatibility, stability, and porous structure that allows tissue ingrowth of host tissues to promote strong anchorage to the implantation site [8-11]. Unlike HA, porous polyethylene has high fracture toughness and ductility, which enable it to be shaped and deformed to fit the contour of defects without breakage. Different types of porous polyethylene are commercially available under the trade names of Medpor or SynPor in several preformed shapes for various applications, and their *in vitro* and *in vivo* performance might be different due to the use of different processing techniques [12]. Apart from commercial porous polyethylene, a combination of 3-dimensional (3D) printing and a wet-salt-bed heat treatment technique was developed to produce a new porous polyethylene implant with greater porosity and pore interconnectivity [13,14]. This new form of porous polyethylene has been investigated for use in ocular implants and for cranioplasty procedures, in which it has shown tissue integration ability for both soft tissue and bone [13,15]. Currently, the intraoral use of porous polyethylene implants remains limited, although it was recently employed as bone graft containment for ridge preservation [16]. Therefore, it was hypothesized that this porous polyethylene could be employed as a bone graft for alveolar or mandible augmentation.

Conducting an animal study to investigate this issue is a crucial step that should be carried out to evaluate the safety, biocompatibility, and performance of the implant prior to clinical investigations. The aim of this study was, therefore, to quantitatively evaluate the effectiveness of porous polyethylene blocks as onlay bone grafts in the posterior mandible of a rabbit model in terms of tissue reaction, bone ingrowth, fibrovascularization, and graft-bone interfacial strength. The knowledge gained from this study is expected to be beneficial

https://doi.org/10.5051/jpis.2020.50.2.106

for broadening our current knowledge and justifying the use of porous polyethylene as a bone graft, especially for alveolar ridge or mandible regeneration. This study is also expected to shed light on the advantages and disadvantages of this material, as well as the precautions that should be taken when clinically applying this material as a bone graft.

MATERIALS AND METHODS

Porous polyethylene fabrication

The same formulation and heat treatment techniques as in previous studies [13-15] were employed to fabricate the porous polyethylene used in this study, except that the preformed shape was produced by using a mold instead of a 3D printing technique. High density polyethylene (HDPE) (Thaizex 7000F, Bangkok Polyethylene Co., Ltd., Bangkok, Thailand) pellets were ground to achieve a mean particle size of approximately 305 μm microns as determined by a Mastersizer (Malvern Instruments, Malvern, UK), and mixed with binders including maltodextrin (Shandong Duqing, Inc., Heze, China) and polyvinyl alcohol (Sigma Aldrich, St. Louis, MO, USA), which were supplied in powder form with particle sizes in the range of 80–100 μm. The mixing ratio was 30% w/w of binder and 70% w/w of HDPE powder. Then, 1.76 g of the mixture was loaded into a rectangular brass mold with cavity dimensions of 80 mm × 4 mm × 10 mm and heated at 145°C for 1 hour. They were then taken out of the mold, sonicated in deionized water for 24 hours to leach out the binders, cleaned with distilled water, and subsequently heated at 145°C for 2 hours while covered with sodium chloride powder (Prungtip, Thai Refined Salt Co., Ltd, Bangkok, Thailand). They were then sonicated in distilled water and dried. The microstructure of the coated specimens was studied using a scanning electron microscope (SEM; JEOL JSM-5410, JEOL., Ltd, Tokyo, Japan) using an accelerating voltage of 20 kV and a working distance of 20 mm. The specimens were coated by gold sputtering prior to observation. The bulk density of the specimens was determined by dividing the weight of each specimen, which was measured using a digital balance (PB4002-S, Mettler Toledo, LLC, Columbus, OH, USA), by its volume, which was calculated by multiplying the width, length, and thickness of the sample as measured by a Vernier caliper (Mitutoyo Corporation, Kawasaki, Japan) with a reading resolution of 0.01 mm. The porosity was calculated from the bulk density of porous polyethylene and the density of solid HDPE (956 kg/m^3) using the following equation:

$$\text{Porosity (\%)} = 1 - \frac{\text{density of porous polyethylene}}{\text{density of solid polyethylene}} \times 100$$

Animal experiment

The animal experimental protocol was reviewed and approved by the Institutional Animal Care and Use Committee of Khon Kaen University (AEKKU 46/2556). Twelve New Zealand white rabbits weighing approximately 3.4 kg were used in this study and randomized into 3 treatment groups according to the study period (4, 12, and 24 weeks). All procedures were performed aseptically under general anesthesia, which was induced by performing an intramuscular injection of a mixture of ketamine hydrochloride (20 mg/kg, Calypsol®, Gedeon Richter Plc, Budapest, Hungary) and xylazine hydrochloride (3 mg/kg, X-Zine®, L.B.S. Laboratory Ltd., Part., Bangkok, Thailand) at a ratio of 5:1. The level of anesthesia was maintained during the operation by 2% isoflurane inhalation (Aerrane®, Baxter Healthcare Corporation, Deerfield, IL, USA). In addition, carprofen (4 mg/kg, Rimadyl®, Pfizer Inc., New York, NY, USA) and tramadol hydrochloride (3 mg/kg, Vesnon-V100®, Vesco Pharmaceutical

https://doi.org/10.5051/jpis.2020.50.2.106

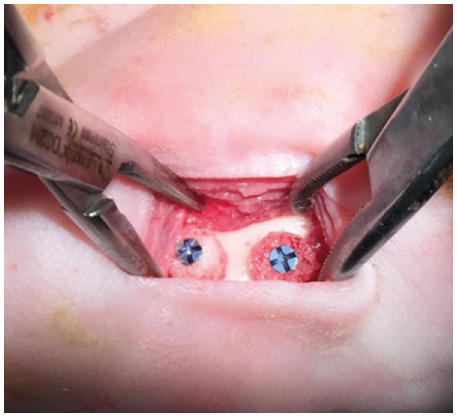

Figure 1. The onlay bone graft implantation procedure in which the cylindrical specimens were directly fixed on the mandible body of the rabbit by a titanium screw.

Co., Ltd, Bangkok, Thailand) were intramuscularly injected, and enrofloxacin hydrochloride (10 mg/kg, Baytril®, Bayer AG, Leverkusen, Germany) was subcutaneously injected prior to the operation. The skin under the border of the mandibular area of each rabbit was shaven and the surgical field was prepared with an iodine solution. A 25-mm incision was then made on the border of the mandible and the periosteum was reflected laterally to expose the body of the mandible. A cylindrical specimen measuring 5 mm in diameter and 4.5 mm in thickness was placed directly on the body of the mandible without bone bed decortication and fixed in place with a titanium screw (1.2 mm in diameter and 7 mm in length) (Figure 1). The specimen was covered with a collagen membrane (FormaAid®, Maxigen Biotech Inc., Taoyuan City, Taiwan) and the incision was closed with 3-0 polyglactin 910 sutures (Vicryl®, Johnson & Johnson, New Brunswick, NJ, USA). Postoperatively, carprofen (4 mg/kg, Rimadyl®, Pfizer Inc.), tramadol hydrochloride (3 mg/kg, Vesnon-V100®, Vesco Pharmaceutical Co., Ltd) and enrofloxacin hydrochloride (10 mg/kg, Baytril®, Bayer AG) were given daily for 7 days. Blood was drawn from each animal preoperatively and at 4 weeks, 12 weeks, and 24 weeks postoperatively to evaluate systemic inflammation and infection. Visual observations of animal conditions and soft tissue healing were made daily. After reaching the end of the specified period, the rabbits were euthanized with an intravenous overdose of barbiturate. The mandible was dissected *en bloc* and further resected at 1 cm from each side of the specimen with a micro motor bur and placed in 10% buffered formalin.

Interfacial shear strength test

The mandible section was secured on the lower platen of the universal testing machine (55R4502, Instron Corporation, Norwood, MA, USA) by a clamping plate to position the interface between the porous polyethylene graft and the mandible in a vertical direction that was parallel to the loading axis of the testing machine. A shear test was done by applying a compressive load at the interface using a mono-beveled chisel-shaped metallic rod attached to the upper movable crosshead of the testing machine using a crosshead speed of 1 mm/min. The maximum load required to detach the specimen from the mandible was recorded, and the shear strength was calculated by dividing the maximum force by the surface area of the specimen. The fracture surfaces of both the bone side and graft side were analyzed by a SEM (s3400N, Hitachi High-Technologies Corporation, Tokyo, Japan) using an accelerating voltage of 10 kV. All specimens and mandibles were coated by gold sputtering prior to observation. Elemental analysis of the fracture surfaces of the porous polyethylene side was performed using energy-dispersive X-ray spectroscopy (EDS, EDAX Inc., Leicester, UK).

https://doi.org/10.5051/jpis.2020.50.2.106

Histologic and histomorphometric analyses

Mandible sections with a porous polyethylene onlay graft were decalcified by 10% formic acid for 48 hours, dehydrated by 95% ethanol for 3 hours (Microm STP 20-3, Thermo Scientific, Dreieich, Germany), and embedded in paraffin (Microm EC 350 Embedding Center, Thermo Scientific). Sections were cut into thin slices using a microtome (Leica RM 2125RT, Thermo Scientific) and stained with hematoxylin and eosin (H&E; Varistain Gemini NS, Thermo Scientific). Photomicrographs of sections were obtained using a light microscope (Olympus BX53, Olympus, Center Valley, PA, USA) at various magnifications. Sections were examined for tissue ingrowth, new bone formation, cellular activity, and any evidence of tissue reaction at the location of implantation. Histomorphometry was performed to quantify the extent of tissue ingrowth using cellSens standard imaging software (Olympus). To measure ingrowth depth, 3 lines were drawn from the outline of the graft at the mandible to the deepest location of the particular tissue observed on the H&E slices (perpendicular to the outline of the graft). The ingrowth depth was defined as the average length of these lines. Ingrowth percentage was calculated by determining the area occupied by bone (BA), fibrous tissue (FA), and total tissue (BA+FA). The total area of the specimen (TA) was determined, and the pore area (PA) available for ingrowth was calculated by multiplying TA by the porosity of porous polyethylene. Through this process, both the absolute and normalized percentages of ingrowth were calculated using the following equations:

$$\text{Absolute ingrowth percentage} = \frac{\text{BA or FA or BA+FA}}{\text{TA}} \times 100$$

$$\text{Normalized ingrowth percentage} = \frac{\text{BA or FA or BA+FA}}{\text{PA}} \times 100$$

Statistical analysis

All statistical analyses were carried out using SPSS for Windows version 11.5 (SPSS Inc., Chicago, IL, USA). The significance of differences in results according to the implantation period was calculated using analysis of variance and Dunnett T3 *post hoc* testing. *P* values<0.05 were considered to indicate statistical significance.

RESULTS

Macroscopically, the microstructure of the porous polyethylene specimen used in this study displayed particle-bridging porous structures with numerous pores as a result of heat treatment (Figure 2). The pore sizes were approximately 200–500 μm and the porosity of the fabricated porous polyethylene was approximately 63%, which was comparable to a previously prepared sample [13-15]. After implantation, all rabbits tolerated the procedure well and survived throughout the entire duration of the study. They were healthy with good appetites, and no altered behavior or signs of complications were observed. Postoperative visual examination showed no evidence of soft tissue dehiscence, inflammation, or infection at the surgical site. The preoperative and postoperative hematological parameters were within the normal ranges [17] and no significant differences were found among all time points (Table 1).

The histological evaluation of the H&E-stained bone slices showed that the porous polyethylene graft had integrated onto the recipient mandibular bone bed and exhibited tissue-bridge connections (Figure 3A). At all postoperative time points, the host tissues were

https://doi.org/10.5051/jpis.2020.50.2.106

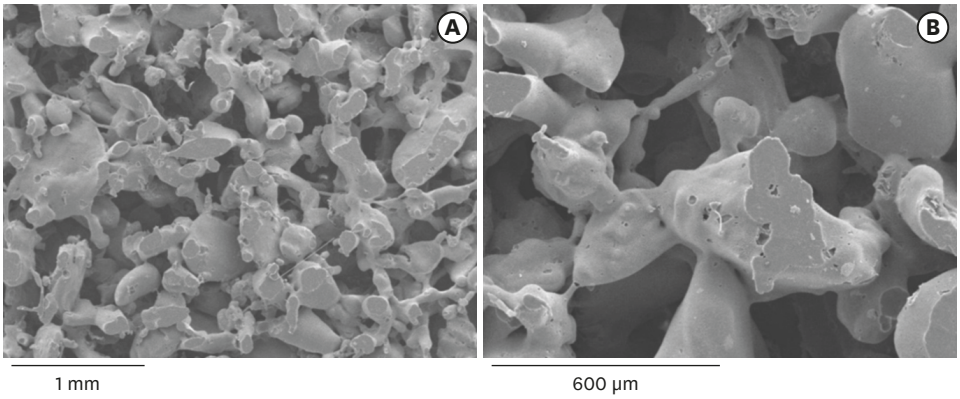

Figure 2. Scanning electron micrographs depicting the microstructure of porous polyethylene. (A) Low magnification. (B) High magnification.

observed to have grown similarly deep into the pores of the porous polyethylene specimens in the direction from the interface to the center of the porous polyethylene graft (Figure 3B-D). Fibrovascular tissue comprising fibrous connective tissue, which was highly rich with collagen fibers and neovessels, was found within the pores (Figure 3E). Some fibrovascular tissue areas were observed to be in the reparative stage, turning into bone through osteoid secretion and mineralization. Generally, new bone ingrowth was mainly observed at the graft-mandibular bone interface, but new bone was also observed to be growing into the pores. This new bone consisted of both immature bone and mature lamellar bone. Lamellar bone was mainly observed in the region near the graft-mandibular bone interface, while immature bone was generally found within the pores, extending deep into the grafts. A lining of osteoblasts at the edge of new bone was also observed, indicating osteoblastic activity in the active bone remodeling process (Figure 3F). A slight inflammatory response was initially demonstrated by the presence of a minimal number of macrophages (approximately 7–8 cells) at 4 weeks postoperatively, but the number of macrophages decreased significantly to 1 or even none at 12 and 24 weeks postoperatively. No multinucleated giant cells or epithelioid cells were detected.

According to the histomorphometric analysis, the absolute and normalized ingrowth percentages of all tissues, which represented the content of ingrowth tissue per total area of the graft and the content of ingrowth tissue per pore spaces respectively, did not significantly differ among the postoperative time points (Table 2). However, the ingrowth percentage of fibrous tissue was significantly greater than that of bone ingrowth at each post-implantation

Table 1. Hematological values of rabbit blood in the pre- and postoperative stages (n=4)

Hematology	Preoperatively		4 weeks postoperatively		12 weeks postoperatively		24 weeks postoperatively	
	Mean±SD	Range	Mean±SD	Range	Mean±SD	Range	Mean±SD	Range
Hemoglobin (g/dL)	13.4±0.4	13.1–13.9	13.1±0.1	13.0–13.2	13.9±0.6	13.5–14.4	12.0±1.3	11.1–12.9
Packed cell volume (%)	41.2±1.7	39.0–43.0	39.0±2.8	37.0–41.0	42.0±2.8	41.0–43.0	38.5±3.5	36.0–41.0
Red blood cell count ($\times10^6$/mL)	6.2±0.4	5.7–6.8	5.8±0.3	5.6–6.1	6.5±0.5	6.2–6.9	5.3±0.8	5.0–6.1
White blood cell count ($\times10^3$/mL)	5.5±0.5	4.9–6.1	7.3±2.6	5.4–9.1	6.2±1.0	5.5–6.9	7.5±2.5	5.7–9.3
Neutrophil (%)	31.5±4.2	26.0–36.0	32.0±2.8	30.0–34.0	35.0±2.1	20.0–50.0	32.5±0.7	32.0–33.0
Lymphocyte (%)	57.5±4.7	51.0–62.0	62.0±1.4	61.0–63.0	47.5±19.1	34.0–61.0	51.5±9.2	45.0–58.0
Basophil (%)	4.5±1.3	3.0–6.0	3.5±2.1	2.0–5.0	8.0±2.8	6.0–10.0	4.0±2.8	2.0–6.0
Monocyte (%)	3.8±2.6	2.0–6.0	4.0±2.8	2.0–6.0	5.5±4.9	2.0–9.0	4.5±3.5	2.0–7.0
Platelets ($\times10^3$/mL)	Adequate		Adequate		Adequate		Adequate	

SD: standard deviation.

https://doi.org/10.5051/jpis.2020.50.2.106

JPIS
Journal of Periodontal & Implant Science

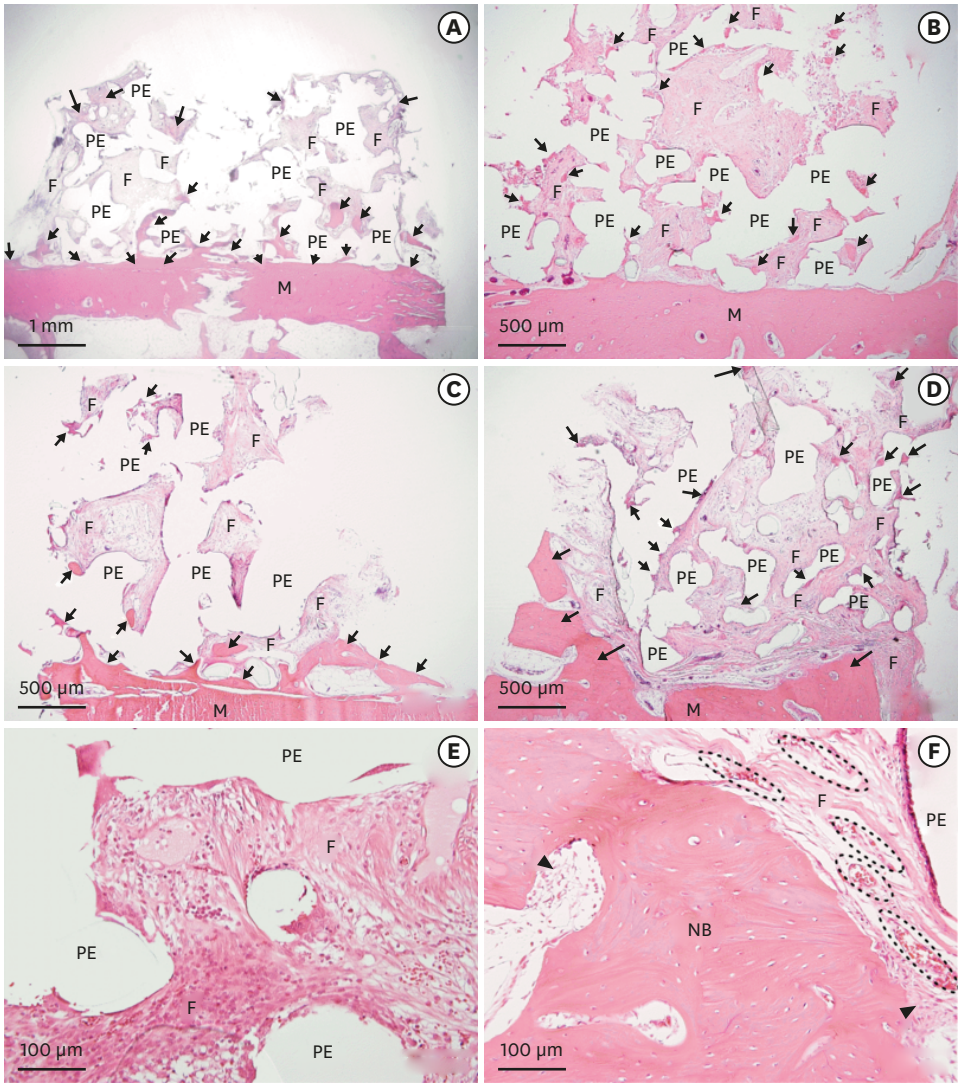

Figure 3. Histological analysis of the ingrowth of tissues in porous polyethylene after it was onlay-grafted on rabbit mandible. Hematoxylin and eosin staining demonstrates the ingrowth of NB (arrows or NB) and F in the pores of PE. (A) Gross appearance. (B) Four weeks after implantation. (C) Twelve weeks after implantation. (D) Twenty-four weeks after implantation. (E) Enlarged view of fibrous tissue with abundant blood vessels growing into the pores of porous polyethylene. (F) Enlarged view of the ingrowth of NB displaying an oriented lamellar structure and a lining of osteoblasts (arrow heads) at the edges. The dotted oval line indicates blood vessels. NB: new bone, F: fibrous tissue, PE: polyethylene.

time point. The depth of fibrous tissue and bone ingrowth tended to increase with time, but significant differences were found between 4 weeks and 12 weeks for fibrous tissue and between 12 weeks and 24 weeks for both fibrous tissue and bone (Figure 4). The interfacial

Table 2. Absolute and normalized ingrowth percentage of total tissue, fibrous tissue and bone at each period after implantation (n=3)

Periods after implantation (wk)	Total tissue ingrowth percentage (%)		Fibrous tissue ingrowth percentage (%)		Bone ingrowth percentage (%)	
	Absolute	Normalized	Absolute	Normalized	Absolute	Normalized
4	36.4±2.8	58.0±4.4	30.2±2.5	47.9±4.0	6.20±0.2	9.84±0.3
12	23.0±7.6	36.6±12.2	17.5±5.8	27.8±9.2	5.50±1.8	8.73±2.9
24	30.4±4.5	48.5±7.2	21.3±2.0	32.7±3.2	9.08±3.7	14.4±5.9

Data are shown as mean±standard deviation. No significant differences among periods for total tissue, fibrous tissue and bone were found (P=3.18, P=6.32, and P=1.27, respectively).

https://doi.org/10.5051/jpis.2020.50.2.106

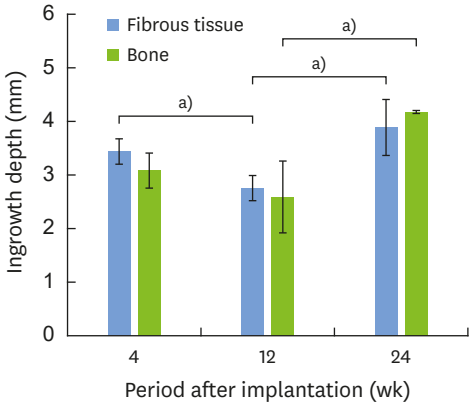

Figure 4. Ingrowth depth of fibrous tissue and bone from the implant-mandibular bone interface into porous polyethylene at each time point after implantation (error bars= standard deviation, n=3). No significant differences were found between 4 weeks and 24 weeks for fibrous tissue, between 4 weeks and 12 weeks for bone, or between 4 weeks and 24 weeks for bone (*P*=0.414, *P*=0.437, and *P*=0.222 respectively).
[a)]Significant difference, *P*<0.05.

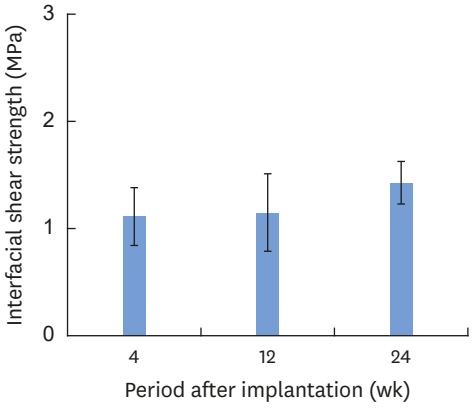

Figure 5. Shear strength of the implant-mandibular bone interface at each time point after implantation (error bars=standard deviation, n=2). No significant differences among time points were found (*P*=0.270).

shear strength of the porous polyethylene at tended to increase over time after implantation, but no significant difference was found among all time points (Figure 5). Analysis of the fracture surface of the porous polyethylene side after shear testing revealed that the porous microstructure of the porous polyethylene was intact and its pores were fully filled by host tissue, without any residual free pore spaces (Figure 6). Numerous elongated tissue fibrils resulted from deformation, and breakage of tissue resulted from the detachment between the graft and the mandible; these features were clearly observed at all post-implantation time points (Figure 6A, C, and E). At 24 weeks, yielding and deformation of the polyethylene structure due to breakage was also observed in some areas in addition to tissue deformation (Figure 6E). The EDS analysis showed that calcium-rich areas were scattered throughout the fracture surface of the porous polyethylene, indicating the presence of residual bone fragments that grew in the pores of the graft (Figure 6B, D, and F). On the surface of the bone side, the location of the fixation of the graft on the mandible was clearly evidenced (Figure 7). The surface of the grafted area was more irregular than the surface of the recipient mandibular bone bed outside, which was relatively smooth. This irregularity resulted from the residual ingrowth tissue that remained on the bone bed after testing.

https://doi.org/10.5051/jpis.2020.50.2.106

JPIS
Journal of Periodontal & Implant Science

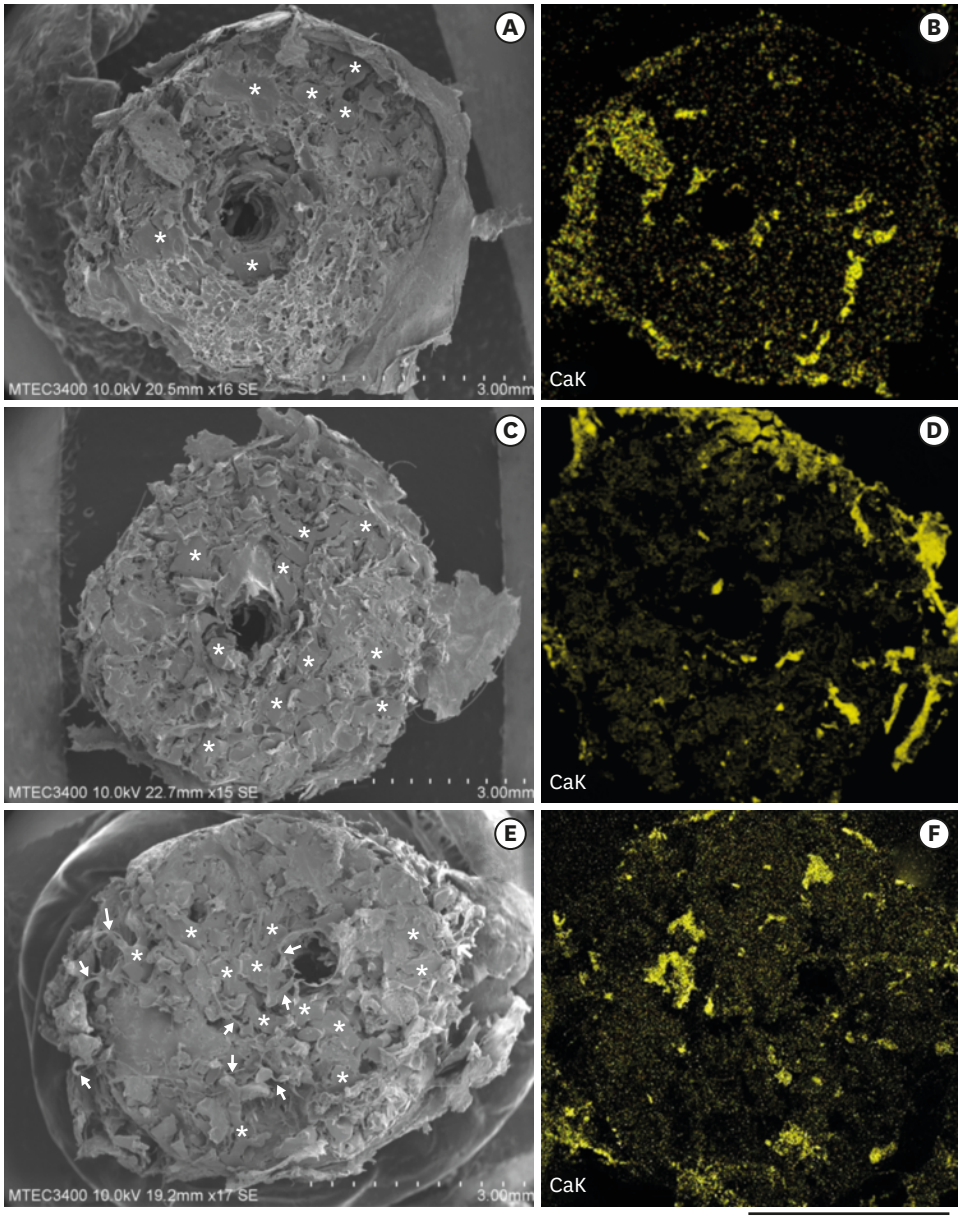

Figure 6. Representative SEM and their corresponding EDS mapping images of elemental calcium on the fracture surfaces of the porous polyethylene side after interfacial shear testing. Evidence is shown of ingrowth of tissue into the pores of polyethylene (*) and elongation of the tissue due to the breakage. Some yielding and deformation of the polyethylene structure due to the breakage is also observed (arrows). (A) SEM, 4 weeks after implantation. (B) EDS mapping image, 4 weeks after implantation. (C) SEM, 12 weeks after implantation. (D) EDS mapping image, 12 weeks after implantation. (E) SEM, 24 weeks after implantation. (F) EDS mapping image, 24 weeks after implantation.
SEM: scanning electron microscope, EDS: energy-dispersive X-ray spectroscopy.

The extent of the irregularities associated with ingrowth tissue increased over time after implantation (Figure 7A-C), but it was difficult to distinguish between the fibrous tissue and bone. However, new bone formation encompassing the outer surface of the porous polyethylene implant was also noted at 12 and 24 weeks postoperatively (Figure 7C).

https://doi.org/10.5051/jpis.2020.50.2.106

JPIS
Journal of Periodontal & Implant Science

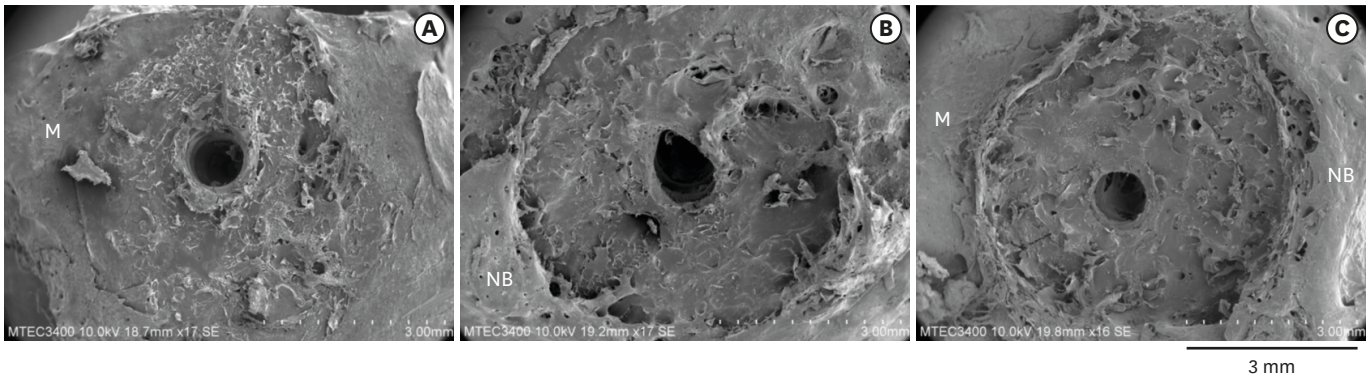

Figure 7. Representative scanning electron micrographs of the fracture surfaces of the mandibular bone side after interfacial shear testing. The location of the fixation of the cylindrical implant on the M is clearly evidenced. NB formation encompassing the outer surface of the porous polyethylene implant is also identified. (A) Four weeks after implantation. (B) Twelve weeks after implantation. (C) Twenty-four weeks after implantation.
M: mandible, NB: new bone.

DISCUSSION

Animal studies of commercial porous polyethylene have previously been conducted in various bone defects [18-25], but the tissue response and ingrowth were generally assessed qualitatively, without quantitative measurements. A low inflammatory response and fibrovascularization into the pores were clearly seen in all previous studies, but contradictory results on bone ingrowth have been reported. Some studies reported the presence of bone ingrowth into the pores of porous polyethylene [18-23], while others reported bone growth far from the porous polyethylene implant [24,25]. The histologic findings regarding bone ingrowth into porous polyethylene implants and graft integration with the recipient bone remain inconclusive. These discrepancies are thought to be due to differences in the animal models and grafting techniques employed in each study, which hinder direct comparisons. In this study, a rabbit mandible model was used to directly represent intraoral mandibular defects, which have a poor blood supply and limited bone marrow, while onlay grafting was used to investigate the osteoconductive and osteogenic properties of porous polyethylene grafts in the absence of influence from the surrounding bone. The tissue ingrowth ability and osseointegration effectiveness of porous polyethylene was investigated through histomorphometric analyses and interfacial strength measurements.

The results of this study demonstrated that the new porous polyethylene block graft could successfully integrate with the recipient mandibular bone bed through the ingrowth of both fibrovascular tissue and new bone. The majority of new bone ingrowth was confined to locations near the graft-bone bed interface, while a lower content of new bone was found in the pores deep in the graft. The large amount of bone neoformation observed near the interface underscores the importance and contribution of native host bone to vascularization and the supply of osteogenic elements in the graft. The native periosteum, which was in direct contact with the graft, could act as a source of osteoprogenitors and as a mineralization front necessary for graft osseointegration [26]. Although bone neoformation was found in the pores of the porous polyethylene, the amount of fibrous tissue ingrowth was still significantly greater than that of new bone, especially in the inner area of the graft. However, the fibrous tissue inside the pores was highly vascularized, which was critical for bone regeneration and osteoconduction. Several areas were also observed to be in the process of transforming into bone and osteoid. The degree of ingrowth of the bone graft into the porous implant is

https://doi.org/10.5051/jpis.2020.50.2.106

known to depend on various factors, including the microstructure of the graft, the movement of the graft, the location of the bone graft, and the preparation of the recipient bone bed. Immobilization of the graft was found to be a crucial factor for bone ingrowth. Bone ingrowth occurred in the presence of small movements, while excessive movements could result in fibrous tissue ingrowth instead [27]. The onlay bone block grafting technique used in this study also represented a challenging situation, since the graft was less exposed to the recipient site vasculature and under the greater forces from the surrounding soft tissues than is the case for inlay grafting [26,28]. Decortication of the bone bed was reported to accelerate bone graft integration with the recipient bed and to induce greater new bone formation at the interface between the bone graft and recipient bed by increasing the vascular supply [29]. Osteogenesis involves the recruitment of mesenchymal stem cells to the site where they differentiate into osteoprogenitors and osteoblasts upon stimulation by local factors [30]. Decortication of the bone bed prior to bone grafting was reported to exert a significant influence on the quantity of new tissue formation and osteogenesis for bone graft integration [29]. Decortication of the bone bed has been found to provide a vascular supply and to place the graft in direct contact with mesenchymal stem cells, osteogenic cells, and cells involved in neovascularization, as well as exposing the graft to the osteoinductive and osteogenic factors present in the blood [31]. Therefore, a decorticated bone bed led to greater new bone formation in the graft than a non-decorticated bed. In this study, although the porous polyethylene block was stabilized with a titanium screw, it might still have been rotated or moved by forces exerted by the soft tissue during mastication. Together with the low vascularization access of the onlay grafting and the non-decortication of the mandibular bone bed, this could have resulted in a lower degree of bone ingrowth than in a defect model in which the implant was fully inserted into the defect, where the graft was surrounded by native bone, was not subjected to forces, and did not move. However, even under these less than optimal conditions, the fabricated porous polyethylene still showed good osteoconductive properties, enabling it to serve as a scaffold for osteogenesis inside the pores and on intraoral surfaces. In addition to the vertical tissue ingrowth from the graft-bone interface into the graft, the fracture surface analysis after interfacial shear testing by scanning electron microscopy also revealed the presence of horizontal new bone regeneration from the area outside the contact interface into the outer surface of the graft, producing a bone wall that enclosed the porous polyethylene graft. This would aid in the stabilization of the graft interface and promote increased bone volume around the graft. The cause of this behavior is unknown, and further study is needed to clarify the underlying mechanism and its impact on bone grafting.

From histomorphometry, the absolute and normalized percentage of bone ingrowth in the fabricated porous polyethylene block grafts was found to be 5.50%–8.74% and 9.08%–14.4%, respectively; these values were relatively comparable to the absolute bone ingrowth values (6.34%–10.49%) reported for a porous HA onlay block graft at 4 and 8 weeks postoperatively [32] and even greater than the values of 2%–4.5% and 5%–10% (absolute and normalized percentages, respectively) reported when 3D fiber-deposited porous titanium was onlay-grafted on goat lumbar spine for 12 weeks [33]. Higher values, of 10%–24% and 24%–32%, respectively, were also reported for sintered porous HA that was implanted into the femoral condyle of rabbits at 5 weeks [34], and normalized values of 10%–25% were reported for porous titanium after 6 weeks [35]. These discrepancies can be explained in terms of differences in materials, microstructure, grafting techniques, implant locations, and animal models. Grafts that were fully inserted into well-vascularized or cancellous bone areas resulted in greater bone neoformation than onlay grafting onto an area with poor blood supply or a cortical bone area, as in this study. The fibrous tissue and bone ingrowth depth

https://doi.org/10.5051/jpis.2020.50.2.106

of porous polyethylene increased over time after implantation, especially between 12 weeks and 24 weeks, which is a typical finding for porous bone grafts [32-36]. It was also noted that the tissue ingrowth depth decreased from 4 to 12 weeks, followed by a re-increase at 24 weeks. This might be attributed to differences in the stages of tissue remodeling, as fast ingrowth was seen at an earlier time point (4 weeks), while restructuring in response to stress and strain occurred later (12 and 24 weeks) [33,34]. Furthermore, differences in the responses of individual animals might have also partially contributed to the observed variation. A definitive explanation of these observations could not be confirmed, and further investigation is needed in the future. Overall, the bone ingrowth depth was in the range of 2.76–3.89 mm, which is in the same range—and even greater—than the ingrowth depth of 2 mm shown in porous titanium implants produced by 3D fiber deposition at 12 weeks postoperatively [33].

The degree of fibrous tissue and bone ingrowth also reflected the degree of integrity of the graft-bone interface. Typically, integration caused by bone ingrowth at the interface would yield a greater interfacial strength than that achieved by fibrointegration. The interfacial shear strength of the porous polyethylene grafts was found to be in the range of 1.11–1.43 MPa. These values are similar to the shear strength of 1.12–4.14 MPa found for titanium pins implanted in rat femur and slightly lower than the values of 2.43–7.65 MPa found for magnesium alloy implants [37]. Our results are also comparable to the values of about 2–3 MPa predicted by a finite element analysis for the shear strength of porous titanium ingrown by porous bone [38] and the interfacial tensile strength of a plasma-sprayed HA coating–titanium implant (0.66–1.12 MPa) [39]. In contrast, a porous tantalum-implanted into canine femur showed much greater shear strength (18.5 MPa) [40]. However, comparisons should be made with caution due to differences in geometry, bone properties, and bonding characteristics. Furthermore, it is difficult to judge what level of interfacial strength is sufficient *in vivo*. It could be possible that a stable interface might not require the maximal strength. The shear strength of the porous polyethylene-mandibular bone interface showed a slight increase with implantation time, but no significant difference was found among all time points. This slight increase might have been related to the observed increase in tissue and bone ingrowth depth, especially at 12 and 24 weeks after implantation. However, it has also been shown that the correlation between bone ingrowth depth and strength of the bone-implant interface depended on ingrowth depth only up to a certain point, and would not further increase beyond this value [41]. A finite element study of micro-models also provided support for the proposal that an increase in bone ingrowth depth would not continue to increase the bone-implant interface strength beyond the threshold of ingrowth depth that already yielded maximal strength [38]. A threshold depth of 1.5 mm was obtained in finite element analysis as the value for which maximum tensile and shear strength was achieved. Therefore, the overall nonsignificant difference in interfacial shear strength might imply that the bone ingrowth of porous polyethylene had already passed the threshold limit.

It was concluded that the new porous polyethylene did not show any adverse systemic reactions and could support both fibrovascularization and bone neoformation at the interface and deep within the pores, even when grafting was performed under less than optimal conditions. Histomorphometric analyses and interfacial shear strength testing demonstrated stable interfacial integration between the graft and bone. Further studies in a different model with a larger sample size and clinical trials are still needed to evaluate and ascertain the effectiveness of this new form of porous polyethylene as a material for use in bone grafts for alveolar ridge or mandible augmentation in actual clinical situations.

https://doi.org/10.5051/jpis.2020.50.2.106

ACKNOWLEDGEMENTS

Thaiwah Co., Ltd., Thailand is thanked for the supply of pregelatinized starch. Dr. Kasem Rattanapinyopituk, Department of Veterinary Pathology, Faculty of Veterinary Science, Chulalongkorn University is thanked for helping with the histologic analysis. The Faculty of Science, Mahidol University and the National Metal and Materials Technology Center (MTEC) are acknowledged for their support with instruments used to characterize various materials.

REFERENCES

1. Misch CM. Ridge augmentation using mandibular ramus bone grafts for the placement of dental implants: presentation of a technique. Pract Periodontics Aesthet Dent 1996;8:127-35.
PUBMED
2. Dimitriou R, Jones E, McGonagle D, Giannoudis PV. Bone regeneration: current concepts and future directions. BMC Med 2011;9:66.
PUBMED | CROSSREF
3. Leonetti JA, Koup R. Localized maxillary ridge augmentation with a block allograft for dental implant placement: case reports. Implant Dent 2003;12:217-26.
PUBMED | CROSSREF
4. Lane JM, Sandhu HS. Current approaches to experimental bone grafting. Orthop Clin North Am 1987;18:213-25.
PUBMED
5. Prolo DJ, Rodrigo JJ. Contemporary bone graft physiology and surgery. Clin Orthop Relat Res 1985:322-42.
PUBMED
6. Mercier P. Failures in ridge reconstruction with hydroxyapatite. Analysis of cases and methods for surgical revision. Oral Surg Oral Med Oral Pathol Oral Radiol Endod 1995;80:389-93.
PUBMED | CROSSREF
7. Dewi AH, Ana ID. The use of hydroxyapatite bone substitute grafting for alveolar ridge preservation, sinus augmentation, and periodontal bone defect: a systematic review. Heliyon (Lond) 2018;4:e00884.
PUBMED | CROSSREF
8. Wellisz T. Clinical experience with the Medpor porous polyethylene implant. Aesthetic Plast Surg 1993;17:339-44.
PUBMED | CROSSREF
9. Choi JC, Fleming JC, Aitken PA, Shore JW. Porous polyethylene channel implants: a modified porous polyethylene sheet implant designed for repairs of large and complex orbital wall fractures. Ophthal Plast Reconstr Surg 1999;15:56-66.
PUBMED | CROSSREF
10. Niechajev I. Porous polyethylene implants for nasal reconstruction: clinical and histologic studies. Aesthetic Plast Surg 1999;23:395-402.
PUBMED | CROSSREF
11. Liu JK, Gottfried ON, Cole CD, Dougherty WR, Couldwell WT. Porous polyethylene implant for cranioplasty and skull base reconstruction. Neurosurg Focus 2004;16:ECP1.
PUBMED | CROSSREF
12. Vollkommer T, Henningsen A, Friedrich RE, Felthaus OH, Eder F, Morsczeck C, et al. Extent of inflammation and foreign body reaction to porous polyethylene *in vitro* and *in vivo*. In Vivo 2019;33:337-47.
PUBMED | CROSSREF
13. Suwanprateeb J, Suvannapruk W, Wasoontararat K, Leelapatranurak K, Wanumkarng N, Sintuwong S. Preparation and comparative study of a new porous polyethylene ocular implant using powder printing technology. J Bioact Compat Polym 2011;26:317-31.
CROSSREF
14. Suwanprateeb J, Thammarakcharoen F, Suvannapruk W. Preparation and characterization of 3D printed porous polyethylene for medical applications by novel wet salt bed technique. Chiang Mai J Sci 2013;41:200-12.
15. Suwanprateeb J, Thammarakcharoen F, Rukskul P. Customized three dimensional printed porous polyethylene for calvarial reconstruction. Adv Mat Res 2012;506:477-80.

16. Mandelaris GA, Spagnoli DB, Rosenfeld AL, McKee J, Lu M. Tissue engineering for lateral ridge augmentation with recombinant human bone morphogenetic protein 2 combination therapy: a case report. Int J Periodontics Restorative Dent 2015;35:325-33.
PUBMED | CROSSREF
17. Özkan C, Kaya A, Akgul Y. Normal values of hematological and some biochemical parameters in serum and urine of New Zealand white rabbits. World Rabbit Sci 2012;20:253-9.
CROSSREF
18. Spector M, Flemming WR, Kreutner A, Sauer BW. Bone growth into porous high-density polyethylene. J Biomed Mater Res 1976;10:595-603.
PUBMED | CROSSREF
19. Klawitter JJ, Bagwell JG, Weinstein AM, Sauer BW. An evaluation of bone growth into porous high density polyethylene. J Biomed Mater Res 1976;10:311-23.
PUBMED | CROSSREF
20. Sevin K, Askar I, Sabuncuoglu BT, Saray A, Yormuk E. The fate of high-density porous polyethylene Medpor implants inserted into mandibular bone defects of dogs. J Med Res 1999;17:125-7.
21. Oliveira RV, de Souza Nunes LS, Filho HN, de Andrade Holgado L, Ribeiro DA, Matsumoto MA. Fibrovascularization and osteogenesis in high-density porous polyethylene implants. J Craniofac Surg 2009;20:1120-4.
PUBMED | CROSSREF
22. Fouad H, AlFotawi R, Alothman OY, Alshammari BA, Alfayez M, Hashem M, et al. Porous polyethylene coated with functionalized hydroxyapatite particles as a bone reconstruction material. Materials (Basel) 2018;11:E521.
PUBMED | CROSSREF
23. Martínez Rodríguez J, Renou SJ, Guglielmotti MB, Olmedo DG. Tissue response to porous high density polyethylene as a three-dimensional scaffold for bone tissue engineering: an experimental study. J Biomater Sci Polym Ed 2019;30:486-99.
PUBMED | CROSSREF
24. Claro FA, Lima JR, Salgado MA, Gomes MF. Porous polyethylene for tissue engineering applications in diabetic rats treated with calcitonin: histomorphometric analysis. Int J Oral Maxillofac Implants 2005;20:211-9.
PUBMED
25. Kim K, Kim BH, Jung S, Park HJ, Ohk SH, Oh HK, et al. Evaluation of osseointegration ability of porous polyethylene implant (Medpor) treated with chitosan. J Nanomater 2014;2014:415929.
CROSSREF
26. Ghiacci G, Graiani G, Ravanetti F, Lumetti S, Manfredi E, Galli C, et al. "Over-inlay" block graft and differential morphometry: a novel block graft model to study bone regeneration and host-to-graft interfaces in rats. J Periodontal Implant Sci 2016;46:220-33.
PUBMED | CROSSREF
27. Pilliar RM, Lee JM, Maniatopoulos C. Observations on the effect of movement on bone ingrowth into porous-surfaced implants. Clin Orthop Relat Res 1986:108-13.
PUBMED | CROSSREF
28. Titsinides S, Agrogiannis G, Karatzas T. Bone grafting materials in dentoalveolar reconstruction: a comprehensive review. Jpn Dent Sci Rev 2019;55:26-32.
PUBMED | CROSSREF
29. Canto FR, Garcia SB, Issa JP, Marin A, Del Bel EA, Defino HL. Influence of decortication of the recipient graft bed on graft integration and tissue neoformation in the graft-recipient bed interface. Eur Spine J 2008;17:706-14.
PUBMED | CROSSREF
30. Khan SN, Cammisa FP Jr, Sandhu HS, Diwan AD, Girardi FP, Lane JM. The biology of bone grafting. J Am Acad Orthop Surg 2005;13:77-86.
PUBMED | CROSSREF
31. Romih M, Delécrin J, Heymann D, Passuti N. The vertebral interbody grafting site's low concentration in osteogenic progenitors can greatly benefit from addition of iliac crest bone marrow. Eur Spine J 2005;14:645-8.
PUBMED | CROSSREF
32. Bae SY, Park JC, Shin HS, Lee YK, Choi SH, Jung UW. Tomographic and histometric analysis of autogenous bone block and synthetic hydroxyapatite block grafts without rigid fixation on rabbit calvaria. J Periodontal Implant Sci 2014;44:251-8.
PUBMED | CROSSREF

33. Li JP, Habibovic P, van den Doel M, Wilson CE, de Wijn JR, van Blitterswijk CA, et al. Bone ingrowth in porous titanium implants produced by 3D fiber deposition. Biomaterials 2007;28:2810-20.
PUBMED | CROSSREF

34. Galois L, Mainard D. Bone ingrowth into two porous ceramics with different pore sizes: an experimental study. Acta Orthop Belg 2004;70:598-603.
PUBMED

35. Hing KA, Best SM, Tanner KE, Bonfield W, Revell PA. Quantification of bone ingrowth within bone-derived porous hydroxyapatite implants of varying density. J Mater Sci Mater Med 1999;10:663-70.
PUBMED | CROSSREF

36. Baril E, Lefebvre LP, Hacking SA. Direct visualization and quantification of bone growth into porous titanium implants using micro computed tomography. J Mater Sci Mater Med 2011;22:1321-32.
PUBMED | CROSSREF

37. Castellani C, Lindtner RA, Hausbrandt P, Tschegg E, Stanzl-Tschegg SE, Zanoni G, et al. Bone-implant interface strength and osseointegration: biodegradable magnesium alloy versus standard titanium control. Acta Biomater 2011;7:432-40.
PUBMED | CROSSREF

38. Tarala M, Waanders D, Biemond JE, Hannink G, Janssen D, Buma P, et al. The effect of bone ingrowth depth on the tensile and shear strength of the implant-bone e-beam produced interface. J Mater Sci Mater Med 2011;22:2339-46.
PUBMED | CROSSREF

39. Lin H, Xu H, Zhang X, de Groot K. Tensile tests of interface between bone and plasma-sprayed HA coating-titanium implant. J Biomed Mater Res 1998;43:113-22.
PUBMED | CROSSREF

40. Bobyn JD, Stackpool GJ, Hacking SA, Tanzer M, Krygier JJ. Characteristics of bone ingrowth and interface mechanics of a new porous tantalum biomaterial. J Bone Joint Surg Br 1999;81:907-14.
PUBMED | CROSSREF

41. Biemond JE, Eufrásio TS, Hannink G, Verdonschot N, Buma P. Assessment of bone ingrowth potential of biomimetic hydroxyapatite and brushite coated porous E-beam structures. J Mater Sci Mater Med 2011;22:917-25.
PUBMED | CROSSREF

https://doi.org/10.5051/jpis.2020.50.2.106